



## Numerical Analysis of Variable Morphing Wing for Improved Aerodynamic Performance of a Predator MQ-1B

Erdogan Kaygan

<sup>1</sup> Girne American University, Department of Aviation Management and Pilotage, Cyprus, Turkey  
erdogankaygan@gau.edu.tr - 0000-0003-3319-3657



### Abstract

In this paper, aerodynamic performance benefits of morphing unmanned aerial vehicle's wing concepts are investigated. A Predator MQ-1B with variable wing structure was utilized for this study. The concept consists of variable twist ( $-10^\circ < \theta < 10^\circ$ , in steps of  $\pm 2.5^\circ$ ) and wing sweep ( $0^\circ < \theta < 30^\circ$ , in steps of  $+10^\circ$ ) to illustrate morphing wing's performance benefits. All computations were performed with Athena Vortex Lattice modelling with varying degrees of twist and sweep angle considered. The results obtained from this work show that if morphing wings adapted to the Predator MQ-1B, it will provide significant performance benefits and also offer a great opportunity to reduce fuel consumption.

### Keywords

Aerodynamics  
Morphing  
Predator  
Sweep  
Twist

### Time Scale of Article

Received 30 August 2022  
Revised until 19 September 2022  
Accepted 23 September 2022  
Online date 29 December 2022

### 1. Introduction

Unmanned aerial vehicles (UAVs) are the most dynamic field of Aerospace technology which is an emerging technology with a stupendous potential to revolutionize combat and to enable new civilian applications (Austin, 2010; Gundlach, 2012). Although they have been so common in recent years, they have actually been in use for several years. Remotely piloted aircraft first appeared during world war I, but the early efforts were stymied by the primitive guidance technology available. NASA (Kudva, J. et al., 1997), DARPA (Kudva, 2004) and also most of researchers (Abdulrahim et al., 2005; Bourdin, Gatto and Friswell, 2006; Gomez and Garcia, 2011; Prisacariu, Boscoianu and Cîrciu, 2013; Kaygan and Gatto, 2016; Prisacariu, Boşcoianu and Cîrciu, 2017) have been conducted performance studies regarding unpiloted morphing aerial vehicles. (Abdulrahim et al., 2005) designed twist morphing wings and flight tests demonstrate the actuation causes sufficient

deformation of the wing to result in significant control authority. Similarly, (Bourdin, Gatto and Friswell, 2006; Gomez and Garcia, 2011; Prisacariu, Boscoianu and Cîrciu, 2013; Kaygan and Gatto, 2016 ) developed twist morphing wings for roll control and also for performance benefits of an aircraft. According to all studies, approximately 20% performance benefits achieved and similar to the fixed wing – aileron roll control was achieved using twist wing configurations. Morphing aircraft is a unique design concept that has been proposed as a solution to the performance constraints of conventional aircraft. The motivation behind wing morphing comes from the observation of the birds where they alter their wings' configuration to achieve suitable aerodynamic profile for several flight regimes. Though this concept seems new-fangled, applications were developed several years ago. Wing-warping techniques were utilized by the Wright Brothers to control the first powered, heavier-than-air aircraft through suspended cables (Culick, 2003). However, in

\*: Corresponding Author Erdogan Kaygan, erdogankaygan@gau.edu.tr  
DOI: 10.23890/IJAST.vm03is02.0202

today's aviation world, this technique is no longer available and has been replaced by traditional control surfaces such as aileron for roll, elevator for pitch, and rudder for yaw control (McRuer and Graham, 2004). Although these surfaces widely accepted as a conventional control surface, it is a fact that they increase drag dramatically due to generation of flow separation over the wing profile. Accordingly, this is the reason why aerospace industry re-calling morphing application to meet the ever-increasing demands for more efficient, robust, and cost-effective designs. Furthermore, most UAVs have mission profiles that require them to cycle between loitering, cruising, climb and fast descents. Comparing Morphing UAV with commercial airlines (See Fig. 1), traditional aircrafts have difficulties to adapt greatly different dynamic flight regimes (Galantai, 2010). The current and past researches summarized by several researchers (Jha and Kudva, 2004; Weisshaar and Challenge, 2006; Min, Kien and Richard, 2010; Barbarino et al., 2011). Adaptive wing concepts are advantageous because aerial vehicle operate in a wide range of flight conditions (e.g., take-off, climb, cruise with various payloads, descent, and landing), each of which have conflicting requirements and performance metrics. For example, in order to have low fuel consumed cruising, an aircraft wing should be as small as possible with sensible camber whilst, when landing, a large area and high camber are desirable for a low enough speed. This need has been addressed with traditional high-lift systems, which are morphing systems in their own right. Although these conventional systems perform well, they have detrimental effects on aerodynamic performance of an aircraft as they rely on hinged control surfaces which can produce significant flow separation when actuated fully. Technological advancements in recent years have fueled research and development into new mechanisms that allow new configurations to meet each requirement. With the recent development of advanced materials and wider mechanism integration, engineers have managed to develop special materials such as aero-elastic skins that are capable of permitting significant structural modification through elastic deformations (Ying Shan et al., 2008; Barbarino et al., 2014). As is well known concept that morphing skin signifies a major problem for morphing technologies (Gandhi and Anusonti-Inthra, 2008; Thill et al., 2008; Olympio et al., 2010). Instead, very few of the concepts for morphing skin deal with the conflicting problems are requiring a smooth and continuous surface that contains adequate structural compliancy while adequately carrying the aerodynamic loads. Many researchers have already mentioned about the benefits and drawbacks of morphing aircraft in details (Min, Kien and Richard, 2010; Barbarino et al., 2011; Weisshaar, 2013). Moreover, significant number of studies completed using wing/winglet twist, span,

sweep and chamber change (Abdulrahim et al., 2005; Bourdin, Gatto and Friswell, 2007; Falcao, Gomes and Suleman, 2011; Kaygan and Gatto, 2014, 2015, 2016; King, Woods and Friswell, 2015; Kaygan, E., Gatto, 2018; Ulusoy et al., 2019; Kaygan, 2020). It seems that the majority of researchers have concentrate on twist morphing application to eliminate discrete control surface and also to improve aerodynamic performance of an aircraft in all flight regimes. One example of the recent development and application of morphing in high lift devices is the Airbus AlbatrossONE(AIRBUS, 2020). It's a small -scaled, remote controlled airplane implemented with semi-aeroelastic hinger wingtips. These moving wingtips help to combat the effects of turbulence, increase the rate of roll as compared to conventional fixed-wing tips. They also help to reduce drag, that would consequently lower the CO2 emissions. Looking to the future though, the need for more efficient aircraft is expected to remain prevalent, forcing designers to look, once again, at these morphing techniques as a means of improving aircraft operations. Although varied and diverse (Jha and Kudva, 2004), at present, the goal of producing a viable alternative to existing aircraft control methodologies remains elusive. The motivation of this study is to analyze aerodynamic performance of a Predator MQ-1B (Fig. 2) with variable wing concept. The concept consists of variable twist ( $-10^\circ < \phi < +10^\circ$ , in steps of  $\pm 2.5^\circ$ ) and wing sweep ( $0^\circ < \Lambda < 30^\circ$ , in steps of  $+10^\circ$ ) to illustrate morphing wing's performance benefits. Hence, the rest of this paper will express the numerical analysis of selected twist and sweep cases.

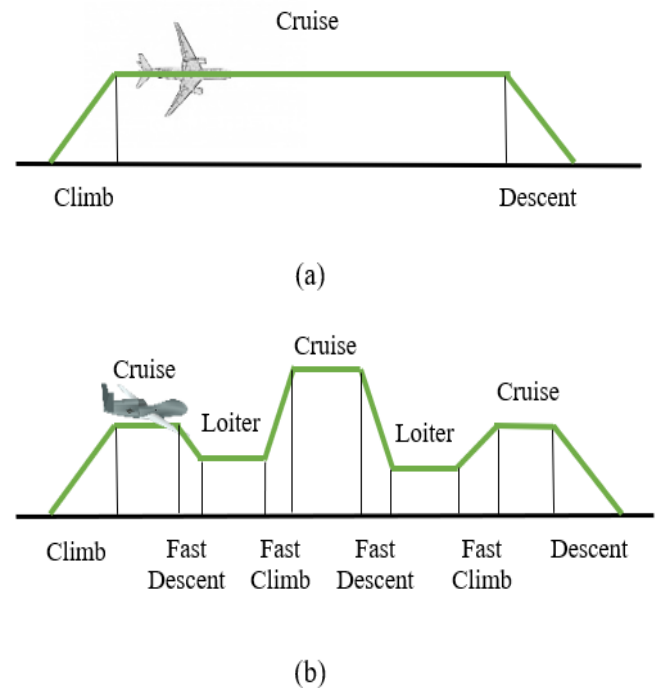


**Fig. 1.** Comparison of mission profiles between; (a) a commercial airliner and (b) surveillance UAV.

## 2 Numerical Method and Analysis

### 2.1. Aircraft flight envelope (gust included)

The MQ-1 Predator wing model chosen for this study (Fig. 4). The MQ-1 Predator is a UAV manufactured by General Atomics for the U.S. Air Force. It is a medium-altitude, long-endurance, and large fixed-wing tactical aircraft (Force., 2009). The main wing configuration

covered a NACA2414 airfoil section (due to low camber, moderate thick and possible use in glider application), and  $1.25^\circ$  leading edge sweep angle, 16.8m wing span, 1.130m root chord, 0.4m tip chord, with aspect and tip ratios of 21.96 and 2.82 respectively. In order to investigate morphing wing performance for dissimilar flight regimes, prearranged values of wing sweep ( $0^\circ < \Lambda < 30^\circ$ , in steps of  $+10^\circ$  as shown in Fig. 6) and twist ( $10^\circ < \phi < 10^\circ$ , in steps of  $\pm 2.5^\circ$  as shown in Fig. 5) are investigated.



Fig. 2. Picture of MQ-1B Predator (Predator, 2015)

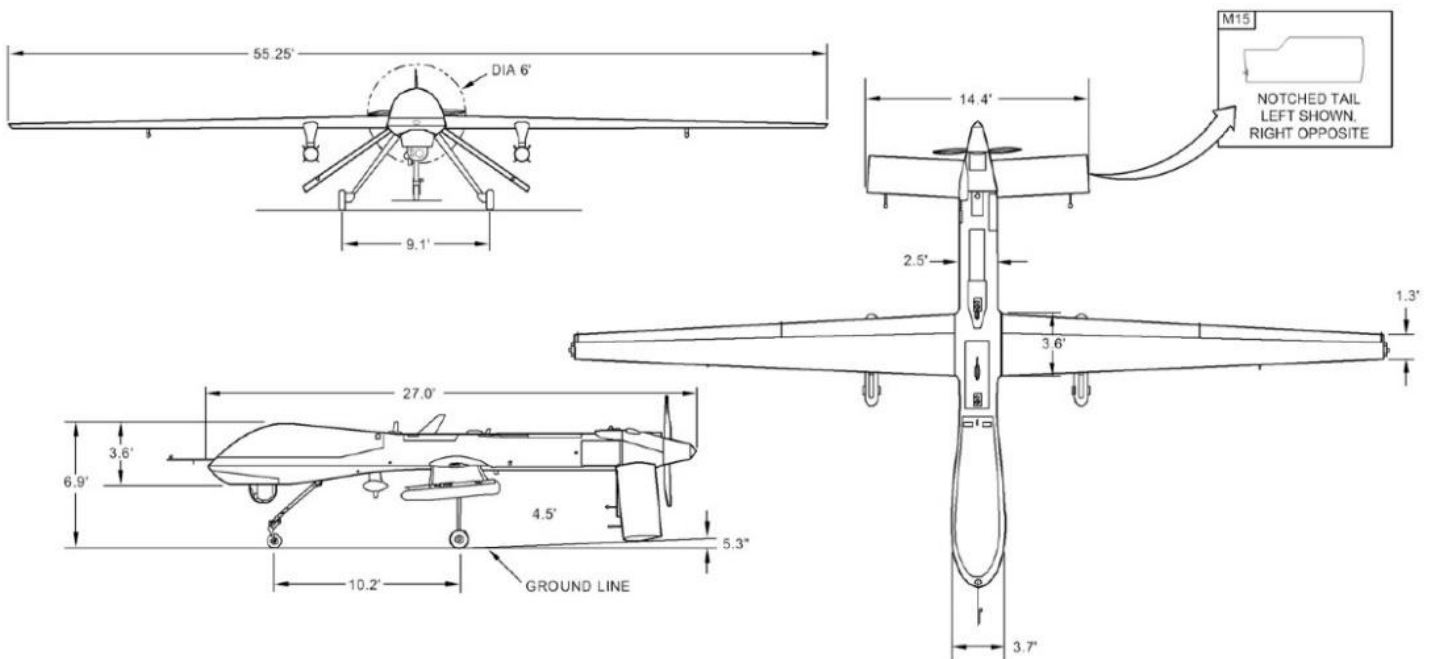


Fig. 3. Design dimensions of MQ-1B Predator UAV (Force., 2009)

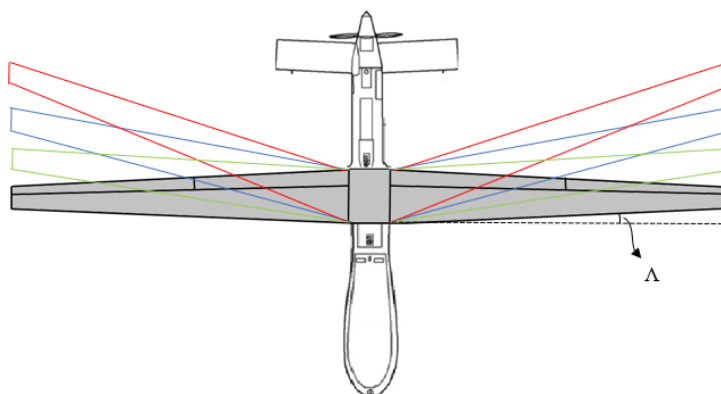
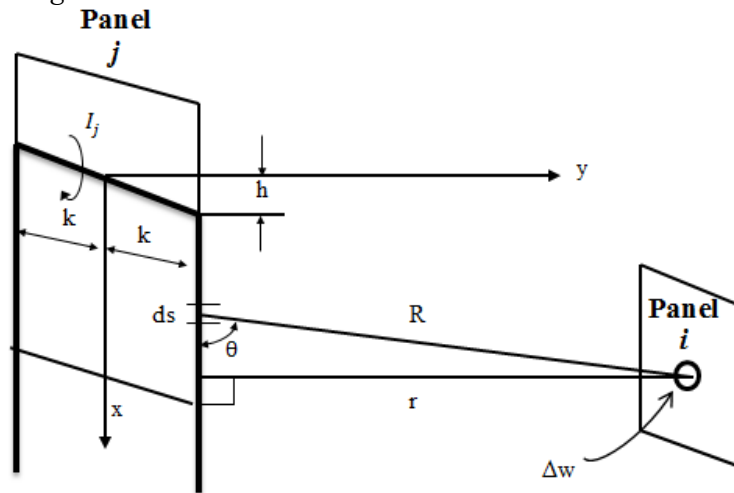


Fig. 4. Sweep wing variations for MQ-1B Predator UAV.

## 2.2. Aerodynamic and Computational Method

The aerodynamic modelling and numerical computations were carried out using Athena Vortex Lattice (AVL) software. Athena Vortex Lattice is a software used to analyze rigid aircraft's aerodynamics and flight dynamics with any configuration. It uses a slender-body model for the fuselages and nacelles and an expanded vortex lattice model for lifting surfaces. It is possible to specify general nonlinear flying states. The entire linearization of the aerodynamic model for any flight state and the specified mass attributes are combined in the dynamic flight analysis. The software mainly utilizes the extended vortex lattice method in obtaining aerodynamic components. For all simulations, a finite number of panels are used to cover the entire wing, as seen in Fig. 7. A series of horseshoe vortices are superimposed such that every panel has a horseshoe vortex represented by a group of letters. The entire wing is covered in a lattice of horseshoe-shaped vortices, each with a different vortex strength. The normal velocity induced by all horseshoe vortices at every control point is determined using the Biot-Savart Law.



**Fig. 5.** Selected panel in three component vortex lines for Vortex Filament Strength

In order to compute the shape changing configuration such as the twist and sweep angle, the relevant aerodynamic panel grids are deflected. This modelling method provides efficient and adequate solutions for the quick determination of the aerodynamic performance of the model being analysed. The vortex strength of the plane is determined by summing the multiplied vortex strength and rotation rates, as well as the velocities through following:

$$I = uI_u + vI_v + wI_w + pI_p + qI_q + rI_r + \delta_e I_{\delta_e} \quad (4)$$

After solving the vortex strength of each panel, the Kutta-Joukowski Law (Saffman, 1992) is applied to obtain the force and moments on each panel over all of the bound vortex segments (Eq 5).

$$dF = \rho U_\infty \times I dl \quad (5)$$

One of the selected panel models is shown in Fig. 5. One of the selected panel models is shown in Fig. 5. For each panel, the same processes are followed to obtain the total vortex strength. The set of simultaneous algebraic equations that form when the flow-tangency condition is applied to all control points can be solved to ascertain the unknown vortex strengths. The velocity at the control point of the panel is calculated by solving the formulas shown in Eq 1. and are the magnitude vectors of and respectively (Eq 2). The influenced matrix is created to solve the required vortex filament strength by multiplying the vortex strength vector and the free stream velocities as illustrated in Eq 3. (Where A is a non-linear function of a matrix depending on the wing shape, b is a vector that can be changed by varying the angle of attack and is the given freestream velocity) (Saffman, 1992).

$$\mathbf{w} = \frac{1}{4\pi} \frac{\mathbf{r}_1 \times \mathbf{r}_2}{|\mathbf{r}_1 \times \mathbf{r}_2|} \left[ \mathbf{r}_0 \cdot \left( \frac{\mathbf{r}_1}{R_1} - \frac{\mathbf{r}_2}{R_2} \right) \right] \quad (1)$$

$$R_1 = \sqrt{(x+h)^2 + (y+k)^2} \quad R_2 = \sqrt{(x-h)^2 + (y-k)^2} \quad (2)$$

$$\mathbf{A} \mathbf{I} = U_\infty \cdot \mathbf{b} \quad (3)$$

The lift force is obtained thereafter by integrating the panel lift distribution. The lift coefficient for a wing can then be calculated using Eq 6.

$$C_L = \frac{L}{\frac{1}{2} \rho V^2 S} \quad (6)$$

Once the wing loading of the structure had been calculated, the variation between the flow angle and freestream velocity for each panel can be obtained. To determine drag force, each panel's lift vector is rotated backwards relative to the freestream direction and integrated as follows:

$$dF = \rho U_\infty \times I dl \sin(\alpha) \quad (7)$$

with the drag coefficient being calculated as;

$$C_D = \frac{D}{\frac{1}{2} \rho V^2 S} \quad (8)$$



(Where  $dF$  is a force acting on an infinitesimal vortex segment,  $\rho$  is an air density,  $I$  is a displacement vector along an infinitesimal vortex segment,  $dl$  is a displacement vector along an infinitesimal vortex segment,  $U_\infty$  and  $V$  are the given freestream velocity) For all simulations, the free-stream velocity was set to 40m/s and all results were calculated without the influence of compressibility. In order to be

computationally efficient, a grid refinement study was performed on the baseline configuration prior to widespread use of the developed model. Based on grid efficiency results, all subsequent computations were based on 20 horseshoe vortices along the wing chord, and 64 along the semi-span of the baseline wing (totally 1280 panels).

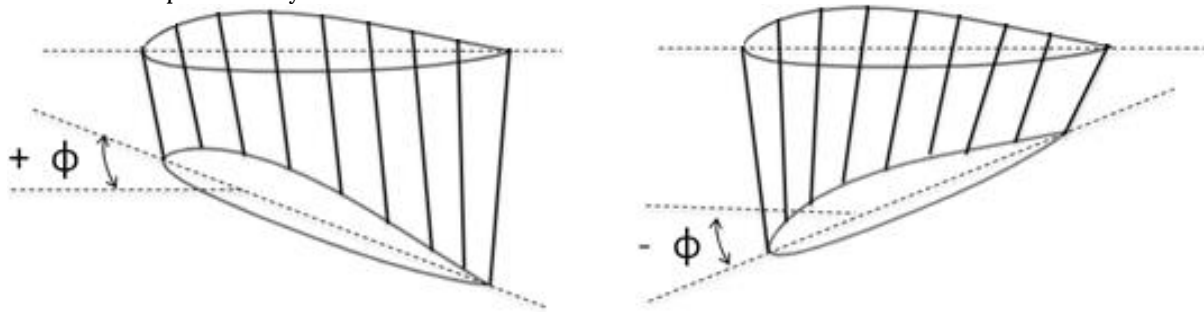


Fig. 6. Schematic view of an active wing: Positive twist angle (washin) and negative twist angle (washout).

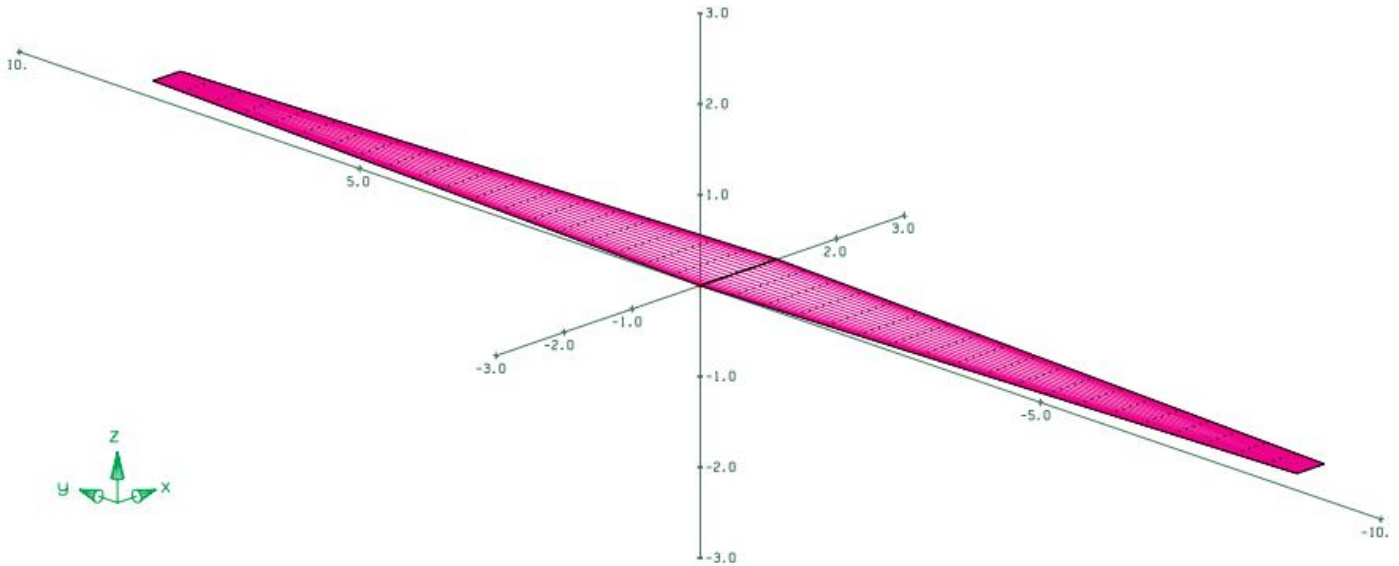


Fig. 7. Athena vortex lattice model morphing wing

### 3. Results and Discussion

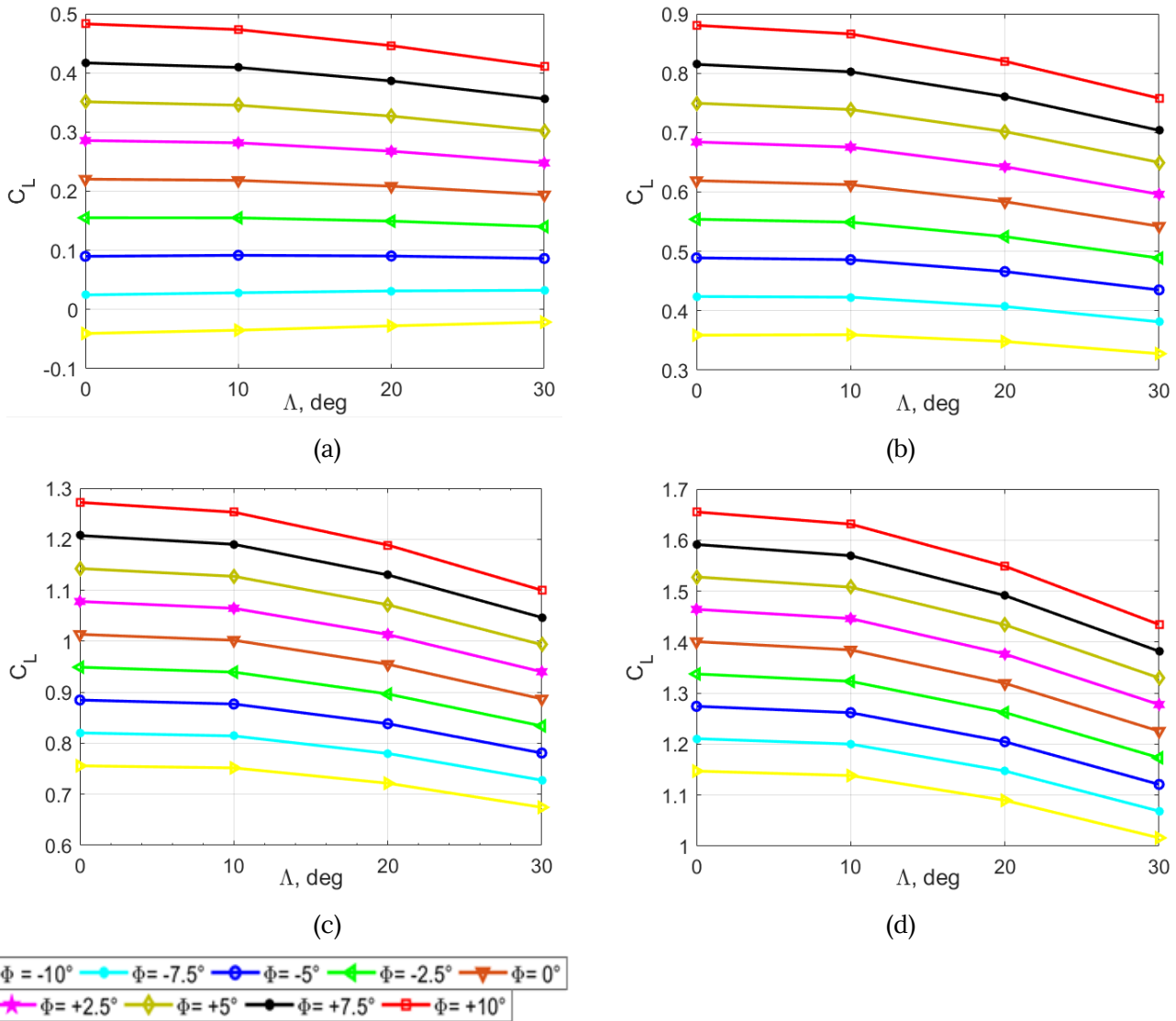
#### 3.1. Effects of Wing Twist and Sweep on Lift and Drag Characteristics of an Aircraft

Fig. 8 shows lift coefficient results for variable twist and sweep cases of an aircraft. It can be seen that increasing or decreasing twist angle of the variable wing producing a corresponding increase and decrease in lift coefficient. Maximum lift obtained at maximum twist angle deflection ( $\phi = +10^\circ$ ) for all variety of  $\alpha$ . This would be expected as increasing positive twist angle cause to increase effective angle of attack of a morphing wing which tends to improve lift production. Considering sweep angle change with twist angle deflection, at  $\alpha=0^\circ$ , is approximately linear with respect to sweep angle for

each twist angle change. As increasing sweep angle to  $30^\circ$ , there will be a reduction in lift coefficient results except for  $\phi = -10^\circ$ , because sweeping a wing backwards tend to take longer for both airflows to travel over the airfoil, resulting in less lift production (Galantai, 2010). Similarly, at  $\alpha=4^\circ$ , with respect to, changing wing sweep angle does have a detrimental effect on lift production with for the most part. Looking through to Fig. 8 (c) and (d), the actuation of the wing twist gives a marked increase in as increasing angle of attack to higher than  $4^\circ$ . Considering flow change at  $\phi = +10^\circ$  from  $\phi = -10^\circ$  contributes positive lift effects approximately 60% (at  $\Lambda=0^\circ$ ). On the other hand, these effects are opposite for sweep angle. Increasing sweep angle reduce lift production as agreement with (Babigian and Hayashibara, 2009). Moreover, for all sweep cases, it can

be seen that reducing twist angle from  $+10^\circ$  to  $-10^\circ$  tends to reduce lift coefficient results as well. This would be expected due to both net reductions in effective angle of attack as the wingtip moves out of the wing plane and contribution to overall lift production reduces (Phillips, 2004). Similar results were found in (Smith et al., 2012) where experimental results present greater for higher positive twist angles Results for drag coefficient (Fig. 9) also show significant changes with wing twist angle change. Initially, at all range of angle of attack, presented results illustrate that wing twisting help to decrease the formation of the wingtip vortices and can be count as a method to alter the load distribution of the wing. Maximum drag coefficient for these conditions were obtained at a maximum twist angle of  $\phi = +10^\circ$  compared to other twist wing configurations. As increasing angle of attack to maximum, results illustrate clear indication for drag reduction in negative twist angles (37.5% and 17.6% at  $\phi = -10^\circ$  comparing to  $\phi = +10^\circ$  and  $\phi = 0^\circ$  respectively).

Proof of this can be seen in the significant number of studies available in the recent works indicating increased downwash angle tends to increase drag coefficient results dramatically (Kaygan and Gatto, 2014; Kaygan and Ulusoy, 2018; Smith et al., 2012). Furthermore, comparing results with angles of attack of  $8^\circ$ ,  $4^\circ$ , and  $0^\circ$ , similar results also be found which showed marked increases at the extremities of twist angles (positive twist) and angles of attack tested as the wing tip becomes more aerodynamically loaded. Due to increased sensitivity to the onset tip flow separation on wing after  $\alpha=4^\circ$ , a dramatic drag increase was seen in most of the positive twist cases presented. A similar trend was observed both computationally and experimentally (Smith et al., 2012) where there is a link between an increment in  $\alpha$  with positive twist variation to a maximum. Considering sweep angle change, drag coefficient seems to be reduced as well. That is the reason why most of the commercial aircrafts have sweep



**Fig. 8.** Effects of changing twist and sweep angle on the lift coefficient ( $C_L$ ): (a)  $\alpha=0^\circ$ , (b)  $\alpha=4^\circ$ , (c)  $\alpha=8^\circ$ , and (d)  $\alpha=12^\circ$ .

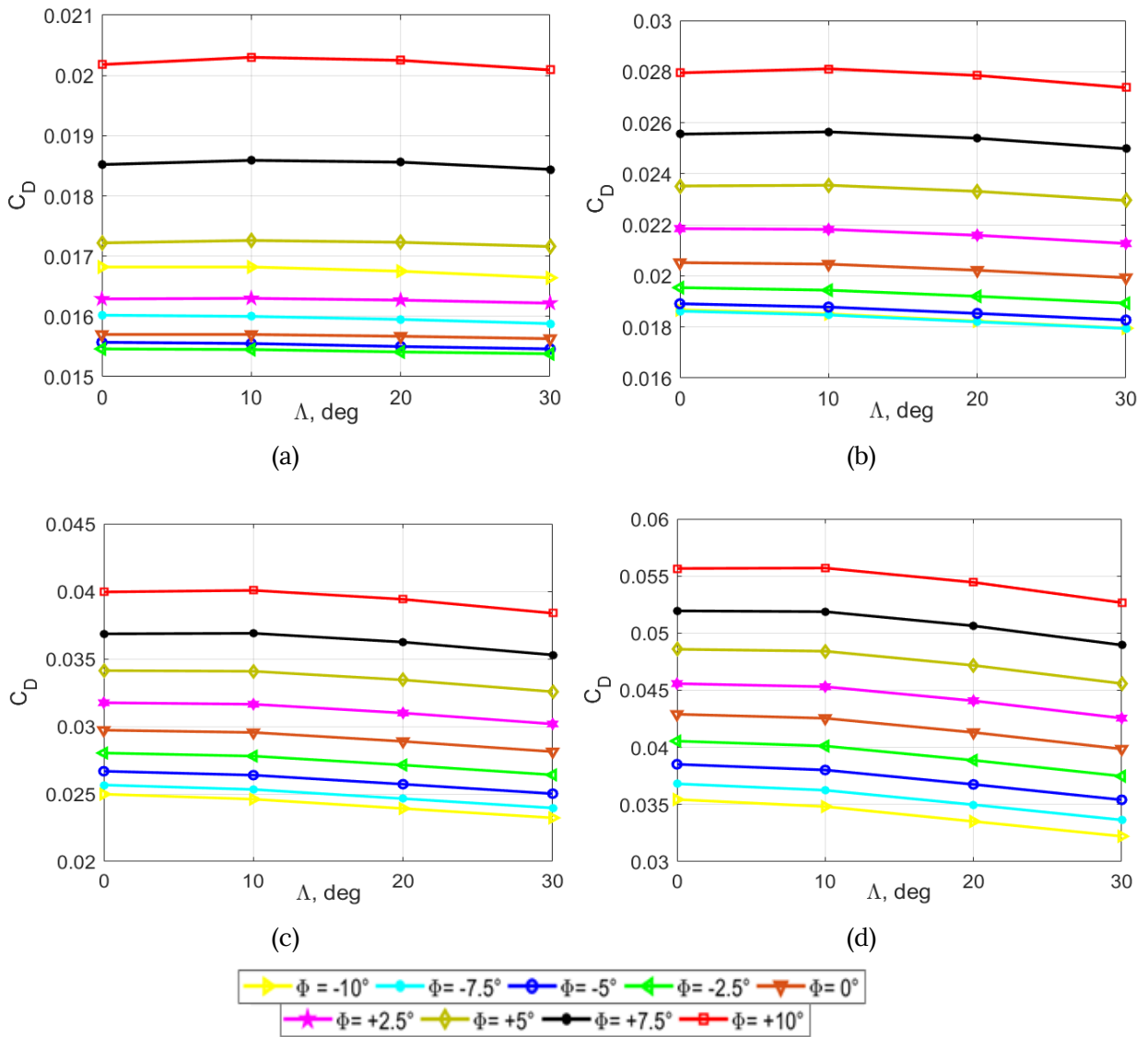


**Fig. 9.** Effects of changing twist and sweep angle on the drag coefficient ( $C_D$ ): (a)  $\alpha=0^\circ$ , (b)  $\alpha=4^\circ$ , (c)  $\alpha=8^\circ$ , and (d)  $\alpha=12^\circ$ .

back wing configuration to reduce fuel consumptions. Maximum drag reduction was found at  $30^\circ$  of sweep,  $\phi = -10^\circ$  at highest angle of attack (40% comparing to  $\phi = +10^\circ$  and  $\Lambda = 0^\circ$ ).

### 3.2. Effects of Wing Twist and Sweep on Aerodynamic Performance of an Aircraft

To summarize the aerodynamic model, Fig. 10 plots Lift to Drag ratio ( $C_L/C_D$ ) versus sweep angles for various of twist angles. As in general flight philosophy, the lift-to-drag ratio of the aircraft initially rise to the maximum, and then reduce as the angle of attack increases. It can be clearly seen Fig. 10 that when the angle of attack comes 3.3. Discussion to  $8^\circ$ , the best maximum lift-to-drag ratio occurs at  $\phi = -2.5^\circ$  and  $\Lambda = 0^\circ$ . Comparing these results with configuration of  $\phi = +10^\circ$  and  $\Lambda = 0^\circ$  and configuration of  $\phi = +10^\circ$  and  $\Lambda = 30^\circ$ , 7% and 6.6% increment were found respectively. Apparently, considering high angles of attack ( $\alpha=12^\circ$ ), the negative twist deflection is favorable to improve the lift-to- drag

ratio characteristics, while the positive deflection has the contradictory effect. When small angles of attacks are concerned ( $\alpha = 0^\circ$ ), it was observed that the wings with positive twist angle contributed more to the aerodynamic performance of the aircraft. The general trend seems to be continued similarly for  $\alpha = 4^\circ$ , although there is a slight difference in positive twist angles (maximum ratio was obtained at  $\phi = +7.5^\circ$ ). In addition to all, sweep angle change also has an effect on the aircraft's performance. As sweep angle increases, there is a reduction in performance for the most cases are simulated, except for  $\Lambda = 10^\circ$ ,  $\phi = -5^\circ$ , and  $\alpha = 8^\circ$ .

### 3.3. Optimized Morphing Wing Twist and Sweep angle

The recommended winglet configurations were selected in base of the augmentations in the aerodynamic performance of an UAV. Five flight profiles (take-off, climb, cruise, descent, and landing) were proposed to utilize as agreement with (Guerrero et al., 2020) and

according to results: During the movement of an aircraft on the ground, it is recommended to use wing sweep angle as high as possible to reduce wingspan of a wing, hence  $\phi = 0^\circ$  and  $\Lambda = 30^\circ$  wing configuration can be used. When aircraft move to take-off stage (1),  $\phi = +10^\circ$  and  $\Lambda = 0^\circ$  wing configuration can be used. In this stage, aircraft needs more lift force to easily take off from runway. Moreover,  $\phi = +10^\circ$  and  $\Lambda = 30^\circ$  wing model is also be used which performs higher lift slope with low drag profile. In stage (2) at the beginning of the climb phase airplane can set the wing position to  $\phi = -5^\circ$  and  $\Lambda = 10^\circ$ . This was taken due to highest lift to drag ratio at high angle of attack. In stage (3), at cruise level where the most of fuel is spending,  $\phi = -5^\circ$  and  $\Lambda = 10^\circ$  wing configurations can be used. Alternatively,  $\phi = -2.5^\circ$  and  $\Lambda = 0^\circ$  can also be used due to low drag value and higher lift to drag ration. If small angle of attack is considered for cruise,  $\phi = -2.5^\circ$

and  $\Lambda = 0^\circ$  would be the best option to reduce fuel consumptions. These configurations sometimes can be changed due to weather conditions, weights and other requirements. Furthermore, increasing twist angle to higher can increase the root bending moments further which may cause adverse effect for aircraft structure. Descents are an essential component of an approach to landing. At this phase (4), lower angle of attack values is concerned. According to the results,  $\phi = -2.5^\circ$  and  $\Lambda = 0^\circ$  or  $\phi = +7.5^\circ$  and  $\Lambda = 0^\circ$  could be used due to lower drag and highest lift to drag ratio. For other small climb and descent segments or sudden altitude changes, as like stage (2) and stage (4) could be use respectively. After landing,  $\phi = 0^\circ$  and  $\Lambda = 30^\circ$  wing configuration can be used. This allows aircraft to reduce wingspan (size) as much as possible to fit regular gates.

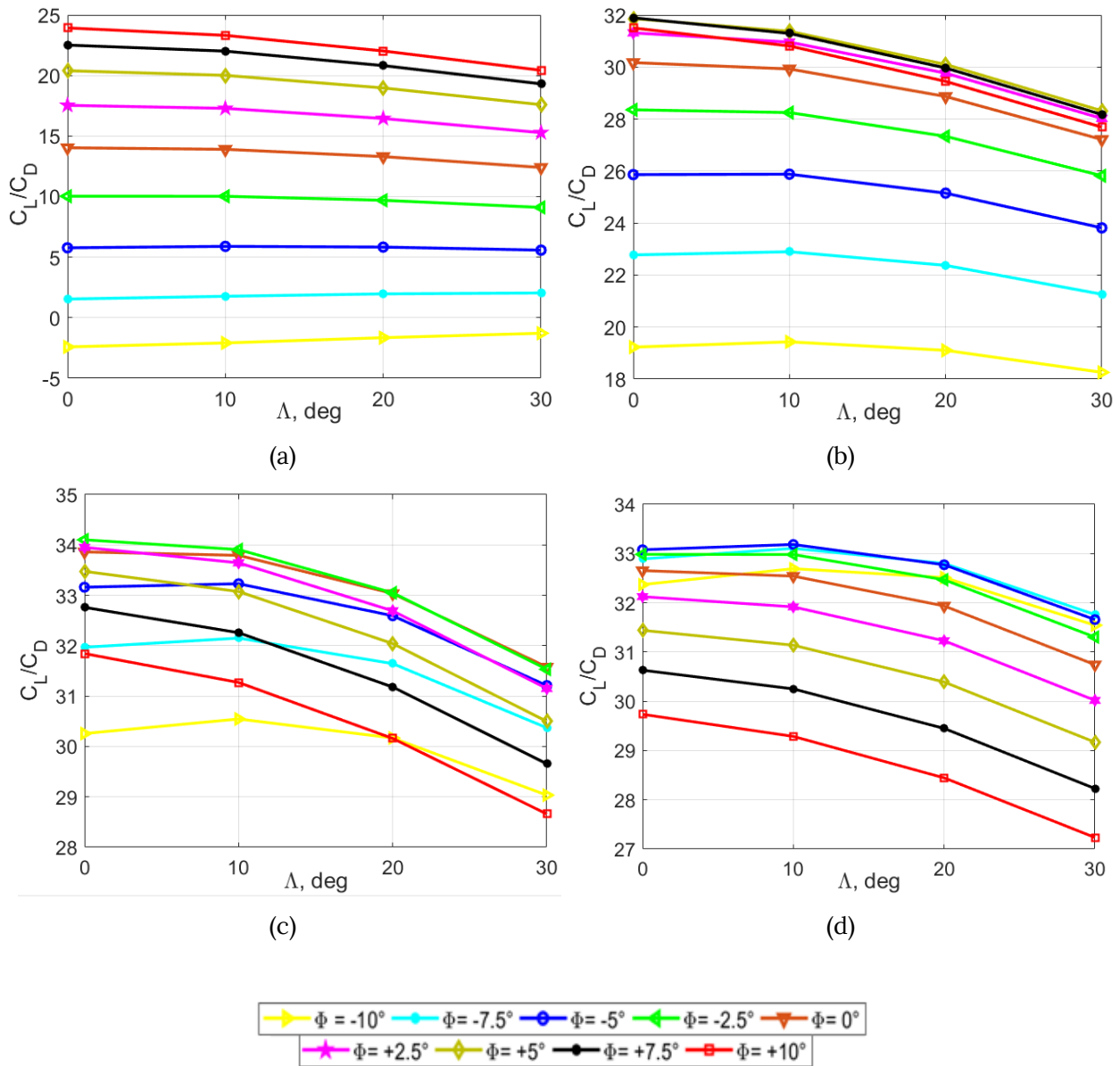


**Fig. 10.** Effects of changing twist and sweep angle on the lift to drag ratio ( $C_L/C_D$ ): (a)  $\alpha = 0^\circ$ , (b)  $\alpha = 4^\circ$ , (c)  $\alpha = 8^\circ$ , and (d)  $\alpha = 12^\circ$ .



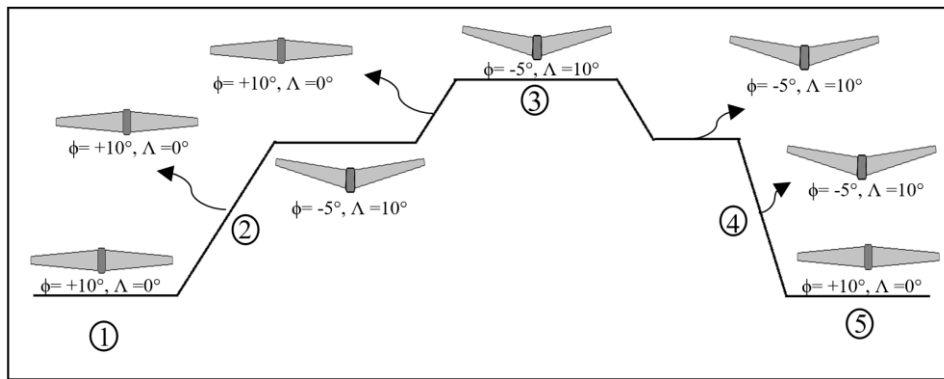


Fig. 11. Optimised Flight Profile

#### 4. Conclusions

The aerodynamic analysis of the variable morphing wing for the Predator MQ-1B was investigated in this paper. From the results, it appears that the overall positive twist configurations have positive effects on lift production and can be applied for flight segments where much more lift is required. In contrast, increasing the negative twist angle to maximum showing lower drag results. Considering the lift/drag ratio, which combines these features, comments can be made about fuel consumption, which is one of the most significant problems related to airlines and general aviation. According to the results, it becomes possible to reduce the fuel cost by adding little sweep angle and also applying negative twist configuration. Overall, the concept demonstrates the possibility of shape changing wing with providing optimum performance benefits. For the future work, the idea of variable wing can be adapted to the UAV and then perform flight tests in order to better understand their effectiveness.

#### Nomenclature

$A$	: Wing Area
$b$	: Wing Span
$C_D$	: Drag coefficient
$C_L$	: Lift coefficient
$C_L/C_D$	: Lift to Drag ratio
$c$	: Wing chord
$i$	: Selected wing panel
$I_i$	: Total vortex strength
$P$	: Density
$U_\infty$	: Freestream velocity
$\alpha$	: Angle of Attack
$\phi$	: Twist Angle
$\Lambda$	: Sweep Angle

#### References

- Abdulrahim, M. et al. (2005) 'Flight Testing A Micro Air Vehicle Using Morphing For Aeroservoelastic Control', *Journal of Aircraft*, 42, No 1(January-February), pp. 1-17. doi:10.2514/6.2004-1674.
- AIRBUS (2020) AlbatrossOne: A revolutionary approach to aircraft wing design. Available at: [https://www.airbus.com/innovation/future-concepts/biomimicry/albatross\\_one.html](https://www.airbus.com/innovation/future-concepts/biomimicry/albatross_one.html) (Accessed: 9 July 2021).
- Austin, R. (2010) *Unmanned Aircraft Systems – UAVs design, development and deployment*. Aerospace series, Wiley and Sons Ltd publication.
- Barbarino, S. et al. (2011) 'A Review of Morphing Aircraft', *Journal of Intelligent Material Systems and Structures*, 22(9), pp. 823-877. doi:10.1177/1045389X11414084.
- Barbarino, S. et al. (2014) 'A review on shape memory alloys with applications to morphing aircraft', *Smart Materials and Structures*, 23(6), pp. 063001--063001. doi:10.1088/0964-1726/23/6/063001.
- Bourdin, P., Gatto, A., and Friswell, M. (2006) 'The Application of Variable Cant Angle Winglets for Morphing Aircraft Control', in 24th Applied Aerodynamics Conference. American Institute of Aeronautics and Astronautics, Inc, pp. 1-13.
- Bourdin, P., Gatto, A. and Friswell, M.I. (2007) 'Potential of Articulated Split Wingtips for Morphing-Based Control of a Flying Wing', in 25th AIAA Applied Aerodynamics Conference, pp. 1-16.
- Culick, F.E.C. (2003) 'The Wright Brothers: First Aeronautical Engineers', 41(6), pp. 8-11.
- Falcao, L., Gomes, A. a and Suleman, A. (2011) 'Design and Analysis of an Adaptive Wingtip', in 52nd AIAA/ASME/ASCE/AHS/ASC Structures, Structural Dynamics and Materials Conference. Denver, Colorado: AIAA.
- Force., D. of A. (2009) 'Airfield Planning and Design

- Criteria for Unmanned Aircraft Systems (UAS)', 4, pp. 1-51.
- Galantai, V.P. (2010) 'Design and Analysis of Morphing Wing for Unmanned Aerial Vehicles', University of Toronto, Canada
- Gandhi, F. and Anusonti-Inthra, P. (2008) 'Skin design studies for variable camber morphing airfoils', *Smart Materials and Structures*, 17(1), p. 015025. doi:10.1088/0964-1726/17/01/015025.
- Gomez, J.C. and Garcia, E. (2011) 'Morphing unmanned aerial vehicles', *Smart Materials and Structures*, 20(10), p. 103001. doi:10.1088/0964-1726/20/10/103001.
- Guerrero, J.E., Sanguineti, M., and Wittkowski, K. (2020) 'Variable cant angle winglets for improvement of aircraft flight performance.' *Meccanica* 55, 1917-1947.
- Gundlach, J. (2012) 'Overview of Unmanned Aircraft Systems', *Designing Unmanned Aircraft Systems*, 2(4), pp. 1-23. doi:10.2514/5.9781600868443.0001.0023.
- Jha, A.K. and Kudva, J.N. (2004) 'Morphing Aircraft Concepts, Classifications, and Challenges'. Edited by E.H. Anderson, 5388, pp. 213-224. doi:10.1117/12.544212.
- Kaygan, A., Gatto, E. (2018) 'Structural Analysis of an Active Morphing Wing for Enhancing Unmanned Aerial Vehicle Performance', *International Journal of Aerospace and Mechanical Engineering*, 12(10), pp. 948-955.
- Kaygan, E. and Gatto, A. (2014) 'Investigation of Adaptable Winglets for Improved UAV Control and Performance', *International journal of Mechanical, Aerospace, Industrial and Mechatronics Engineering*, 8(7), pp. 1281-1286.
- Kaygan, E. and Gatto, A. (2015) 'Computational Analysis of Adaptable Winglets for Improved Morphing Aircraft Performance', *International Journal of Aerospace and Mechanical Engineering*, 9(7), pp. 1127-1133.
- Kaygan, E. and Gatto, A. (2016) 'Development of an Active Morphing Wing With Adaptive Skin for Enhanced Aircraft Control and Performance', in *Greener Aviation 2016*. BRUSSELS, BELGIUM.
- Kaygan E., Ulusoy C. (2018), 'Effectiveness of Twist Morphing Wing on Aerodynamic Performance and Control of an Aircraft', *Journal of Aviation*, 2 (2), 77-87. DOI: 10.30518/jav.482507
- Kaygan E. (2020), 'Aerodynamic Analysis of Morphing Winglets for Improved Commercial Aircraft Performance', *J. Aviat.*4 (1), 31-44.
- King, B., Woods, S. and Friswell, M.I. (2015) 'The Adaptive Aspect Ratio Morphing Wing: Design Concept and Low Fidelity Skin Optimization', pp. 1-4.
- Kudva, J. N., Martin, C. A., Scherer, L. B., Jardine, A. P., McGowan, A. R., Lake, R. C., Sendekyj, G. P., and Sanders, B.P. (1997) 'Overview of DARPA/AFRL/NASA Smart Wing Program', in Jacobs, J.H. (ed.). Bellingham, WA: SPIE Proceedings, pp. 230-236.
- Kudva, J.N. (2004) 'Overview of the DARPA Smart Wing Project', *Journal of Intelligent Materials Systems and Structures*, 15(4), pp. 261-267. doi:10.1177/1045389X04042796.
- McRuer, D. and Graham, D. (2004) 'Flight Control Century: Triumphs of the Systems Approach', *Journal of Guidance, Control, and Dynamics*, 27(2), pp. 161-173. doi:10.2514/1.4586.
- Min, Z., Kien, V.K. and Richard, L.J.Y. (2010) 'Aircraft morphing wing concepts with radical geometry change', *IES Journal Part A: Civil and Structural Engineering*, 3(3), pp. 188-195. doi:10.1080/19373261003607972.
- Olympio, K.R. et al. (2010) 'Design of a Flexible Skin for a Shear Morphing Wing', *Journal of Intelligent Material Systems and Structures*, 21(17), pp. 1755-1770. doi:10.1177/1045389X10382586.
- Phillips, W.F. (2004) 'Lifting-Line Analysis for Twisted Wings and Washout-Optimized Wings. ' *Journal of Aircraft* vol. 41, no. 1 128-136.
- Predator, M.-1 (2015) MQ-1 Predator Air Force Photos. Available at: <https://www.af.mil/News/Photos/igphoto/2000597903/mediaid/4705/> (Accessed: 16 June 2021).
- Prisacariu, V., Boscoianu, M. and Cîrciu, I. (2013) 'Morphing wing concept for small UAV', *Applied Mechanics and Materials*, 332(July), pp. 44-49. doi:10.4028/www.scientific.net/AMM.332.44.
- Prisacariu, V., Boşcoianu, M. and Cîrciu, I. (2017) 'The effect analysis of the morphing concept on the small swept flying wings', *MATEC Web of Conferences*, 121, pp. 1-8. doi:10.1051/mateconf/201712101011.
- Babigian R., Hayashibara, S. (2009), 'Computational Study of the Vortex Wake Generated by a Three-Dimensional Wing with Dihedral, Taper, and Sweep', 27th AIAA Applied Aerodynamics Conference, no. June, pp. 1-13.
- Saffman, P. G. (1992) 'Vortex Dynamics' Cambridge, England, U.K.: Cambridge Univ. Press.
- Smith, D. D., Lowenberg, M. H., Jones, D. P., Friswell, M. I. and Park, S. (2012) 'Computational and Experimental Analysis of the Active Morphing Wing Concept',

2012, pp. 1–9.

Thill, C. et al. (2008) ‘Morphing skins’, (3216), pp. 1–23.

Weisshaar, T. a. (2013) ‘Morphing Aircraft Systems: Historical Perspectives and Future Challenges’, *Journal of Aircraft*, 50(2), pp. 337–353. doi:10.2514/1.C031456.

Weisshaar, T.A. and Challenge, T.H.E.M. (2006) ‘Morphing Aircraft Technology – New Shapes for Aircraft Design’.

Ying Shan et al. (2008) ‘Variable Stiffness Structures Utilizing Fluidic Flexible Matrix Composites’, *Journal of Intelligent Material Systems and Structures*, 20(4), pp. 443–456. doi:10.1177/1045389X08095270.